Generation of Cylindrical Converging Shock Waves in a Conventional Shock Tube

L. Biamino, G. Jourdan, C. Mariani, L. Houas, M. Vandenboomgaerde, and D. Souffland

1 Introduction

For ever two decades, the IUSTI laboratory has been known for its investigations [1] dealing with the Richtmyer-Meshkov instability (RMI). Experiments concerning the RMI have been performed in conventional shock tubes [2, 3, 4, 5]. All these experiments use a planar shock wave to generate the instability as perfectly as possible. However, the RMI also occurs in the spherical case where the convergence effects must be taken into account. As far as we know, no conventional (straight section) shock tube facility has been used to experimentally study the RMI in a spherical geometry. Although the generation of a divergent shock or blast wave is not really experimentally difficult, the production of a well controlled converging shock wave can be harder. Z. Zhai *et al.* [8] have already developed a clever device to realize such a shock wave, but in their solution, it was necessary to create a specific device for each new shock wave velocity.

The present work is the first experimental application of the P.E. Dimotakis and R. Samtaney theory [6], generalized by M. Vandenboomgaerde and C. Aymard [7], that propose to use a suitable shaped interface between two gases of different density. This "hydrodynamical lens" converts the planar shock wave into a cylindrical one which converges along a wedge toward the apex. The described theory is valid for generating either a spherical 3-D converging or a cylindrical 2-D converging shock wave. In the present work, the theory has been exploited and adapted to produce a controlled cylindrical 2-D converging shock wave. The chosen triplet of parameters, i.e., the pair of gases on each side of the interface (air/SF_6), the incident shock wave Mach number (M_{is}=1.15) and the interface's shape (elliptic) generates a perfect convergent cylindrical shock wave. Results from both pressure measure-

L. Biamino · G. Jourdan · C. Mariani · L. Houas
Aix-Marseille Université, IUSTI-CNRS UMR 7343,
5 rue Enrico Fermi, 13013 Marseille, France

M. Vandenboomgaerde · D. Souffland
CEA, DAM, DIF, F-91297 Arpajon, France

R. Bonazza and D. Ranjan (eds.), *29th International Symposium on Shock Waves 2*,
DOI: 10.1007/978-3-319-16838-8_45

ments and schlieren visualizations which allow us to analyse the shape, the velocity and the overpressure evolution behind the converging shock wave propagation confirm the theory.

2 Principle

The purpose of Dimotakis and Samtaney was to use the density difference between two gases to modify the shape of the incident shock wave. For example, when a shock wave initially propagating in ambient air penetrates in SF_6, its velocity is reduced according to the ratio of the acoustic impedance across the air/SF_6 interface, i.e., $W_t < W_i$ where W_i and W_t represent the velocities of the incident and the transmitted shock waves, respectively. By using this property and controlling the interface shape as detailed in Fig. 1, it is possible to bend a shock wave. In order to obtain a convergent cylindrical shock wave, Vandenboomgaerde and Aymard derived the exact equations for the curved interface and proved that its shape is conic. In the case of the studied air/SF_6 gas pair, the shape to impose at the interface is an ellipse with an eccentricity $e = \frac{W_t}{W_i}$.

$$r(\Theta) = r(0)\frac{1-e}{1-e*cos(\Theta)} \tag{1}$$

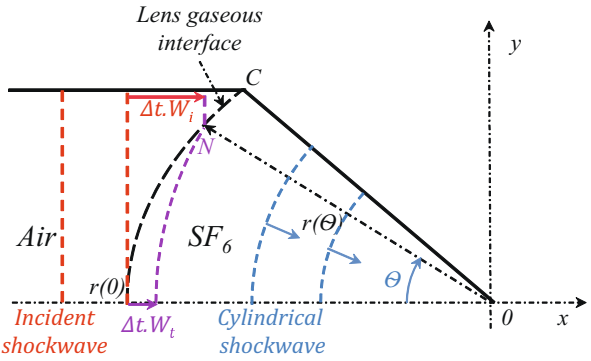

Fig. 1 Sketch of the refraction of a shock wave through a fast-slow shaped interface (air/SF_6)

3 Experiments

Experiments were conducted in a conventional shock tube. The IUSTI's T80 shock tube was chosen for is flexibility and its adaptability. It is an 80×80 mm^2 square cross-section shock tube with the ability to add any extension to the end of its test chamber. Technical details regarding this facility are available in [9]. In the present study, the incident shock wave Mach number was limited to 1.15 into the ambient air. For this study, a new test chamber was designed, manufactured and fitted to

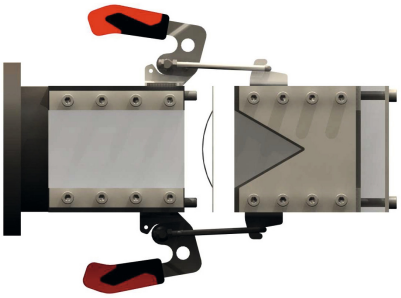

Fig. 2 Virtual representation of the device added at the end of the shock tube to perform the converging cylindrical shock wave

the end of the shock tube. Figure 2 shows a virtual representation of this device. It consists of two sections, one with a constant 80×80 mm^2 square cross-section and another with converging walls. The convergent section is characterized by an apex angle of 60°, an angle large enough to visualize the eventual shock wave's curvature. Between the two sections, a stereolithographied grid was inserted to support a nitrocellulose membrane that separates the two different gases. To assure the gaseous lens function, the grid shape has to be defined by equation (1) as explained above. This grid is unique for these initial conditions, i.e. M_{is}=1.15 and when the gases are air and SF_6 in atmospheric conditions. Changing one of these parameters implies a change of the grid. A schlieren Z-system coupled with a high speed digital camera PHOTRON SA-1 was used to record the wave patterns. The large angle apex imposes a short distance between the gaseous lens and the converging point. Thus, the frame rate chosen to record the sequence was 54000 fps for a spatial resolution of 312×182 pixels. To record the pressure histories during each experiment, seven pressure transducers were set up on the experimental device. Two probes were mounted along the constant section wall to determine the shock wave incident Mach number, the last five were located on the converging walls to analyse the curved shock wave propagation. Implantation of these gauges is visible in Fig.3; the point O is located 4055 mm from the driver section end-wall.

4 Results

Figure 3 is an example of a schlieren picture recorded during the shock wave converging phase. As we can see, the transmitted shock wave is clearly visible and immediately followed by a complex unsteady flow. The convergent shock wave shape is curved and seems to be circular. The circularity was verified as the shock converged towards the apex. By measuring the radius in three different directions (the horizontal, along the upper and the lower walls). Figure 4 presents the reconstructed trajectory of the converging transmitted shock wave issued from the pressure measurement and from the recorded schlieren visualisation. The maximal measurement deviation between the three directions is less than 1.5 mm and can be considered the

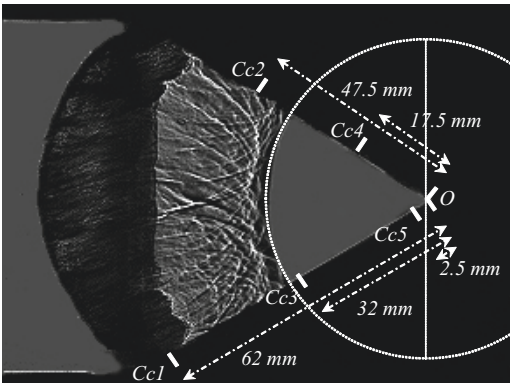

Fig. 3 Schlieren picture of shock wave during its converging phase, Cc1 to Cc5 indicate the location transducers along the wall

measurement error. Over the converging phase, the measured radius along the three directions was identical, suggesting that the shock wave kept a cylindrical shape for the entire period in which it converged. Moreover, in a first stage, we can observe that the transmitted shock wave trajectory is quasi linear. At the end of the converging phase the shock wave deviates from planar trajectory. So, in this stage, the geometrical effects begin to affect the shock wave.

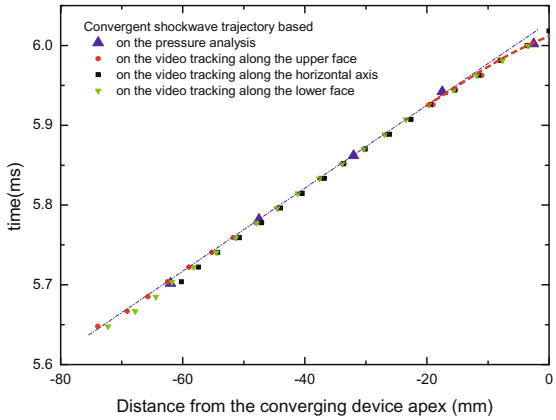

Fig. 4 Reconstruction of the converging shock wave's trajectory: from the pressure measurement and from the recorded schlieren visualisation

The pressure histories are presented in Fig. 5. As expected, the pressure signal recorded behind the incident shock wave in the constant section is the typical signature of a planar shock wave propagation: a sudden rise of pressure followed by a

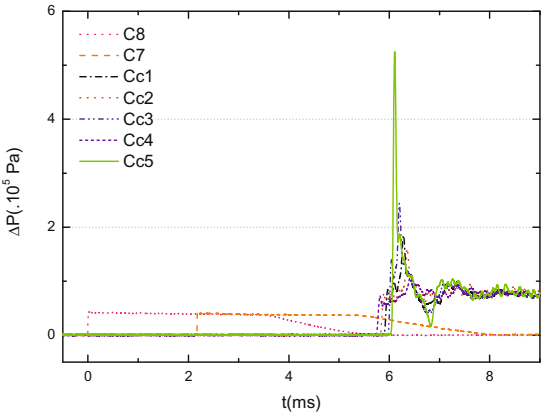

Fig. 5 Overpressure histories recorded along the shocktube (C8, C7) and inside the converging device (Cc1 to Cc5); M_{is}=1.15

plateau. Then, the reflected rarefaction waves from the driver section end-wall reduce pressure. In the convergent section, the pressure levels induced by the transmitted shock wave are higher than those observed before. Moreover, as the convergent shock wave approaches the apex, the pressure level rises. The transmitted shock wave reflection on the convergent apex is also clearly identifiable from stations Cc1 to Cc5. Figure 6 presents the overpressure value obtained behind the converging shock wave versus the distance to the apex. It seems to follow an exponential fit. The overpressure recorded at 2.5 mm before the convergent apex is ten times higher than the one generated by the incident shock wave.

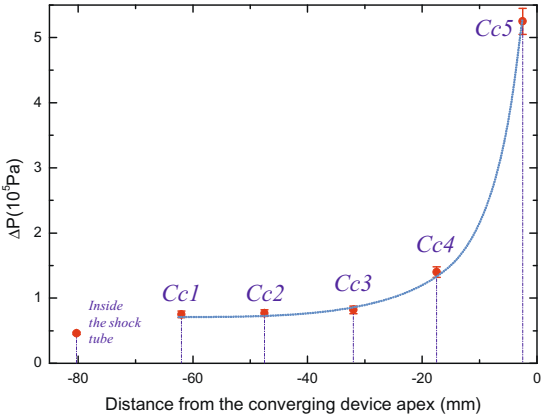

Fig. 6 Overpressure evolution in the converging test section versus the distance from the device apex

5 Conclusion

The present experiment describes a new method to generate a cylindrical convergent shock wave by using a conventional shock tube. Based on the P.E. Dimotakis and R. Samtaney [6] and M. Vandenboomgaerde and C. Aymard [7] theoretical and numerical works, a device have been designed, manufactured and tested. In the case where a planar incident shock wave propagating in air (M_{is}=1.15) refracts through an elliptic air/SF_6 interface it is possible to generate a circular transmitted shock wave. First results from the analysis of sequences of schlieren images and pressure histories clearly indicate that the shock moving in the converging part has a circular shape. Moreover, after the shock refraction through the air/SF_6 elliptic interface, it can be observed from the pressure measurements that the pressure rises sharply after the passage of the transmitted shock and increases gradually due to the shock convergence. Finally, the reconstruction of the transmitted shock wave trajectory shows that the converging shock accelerates during its progression in the convergent test section. Thus, results prove the viability of such a method and lead us to imagine a new field of experimentation on the RMI. In the same way of the previous Mariani et al. work [1], it will be easy to place a complex gaseous interface on the path of such a converging shock wave.

Acknowledgement. This experimental study was supported by the French Atomic Commission (CEA) under contract n° 12-24-C-DSPG/CAJ.

References

1. Mariani, C., Vandenboomgaerde, M., Jourdan, G., Souffland, D., Houas, L.: Investigation of the Richtmyer-Meshkov instability with stereolithographed interfaces. Phys. Rev. Lett. 100(25), 254503 (2008)
2. Meshkov, E.E.: Instability of the interface of two gases accelerated by a shock wave. Fluid Dyn. 4(5), 101–104 (1969)
3. Collins, B.D., Jacobs, J.W.: PLIF flow visualization and measurements of the Richtmyer-Meshkov instability of an air/SF6 interface. J. Fluid Mech. 464, 113–136 (2002)
4. Puranik, P.B., Oakley, J.G., Anderson, M.H., Bonazza, R.: Experimental study of the Richtmyer-Meshkov instability induced by a Mach 3 shock wave. Shock Waves 16(6), 413–429 (2004)
5. Sadot, O., Erez, L., Alon, U., Oron, D., Levin, L.A., Erez, G., Ben-Dor, G., Shvarts, D.: Study of Nonlinear Evolution of Single-Mode and Two-Bubble Interaction under Richtmyer-Meshkov Instability. Phys. Rev. Lett. 80, 1654–1657 (1998)
6. Dimotakis, P.E., Samtaney, R.: Planar shock cylindrical focusing by a perfect-gas lens. Phys. Fluids 18(3), 031705 (2006)
7. Vandenboomgaerde, M., Aymard, C.: Analytical theory for planar shock focusing through perfect gas lens and shock tube experiment designs. Phys. Fluids 23, 016101 (2011)
8. Zhai, Z., Si, T., Luo, X., Yang, J., Liu, C., Tan, D., Zou, L.: Parametric study of cylindrical converging shock waves generated based on shock dynamics theory. Phys. Fluids 24, 026101 (2012)
9. Jourdan, G., Houas, L., Schwaederlé, L., Layes, G., Carrey, R., Diaz, F.: A new variable inclination shock tube for multiple investigations. Shock Waves 13(6), 501–504 (2004)